Nationaal Lucht- en Ruimtevaartlaboratorium
National Aerospace Laboratory NLR

Executive summary

Circular Harmonics Beamforming with multiple rings of microphones

AIAA Paper 2012-2224

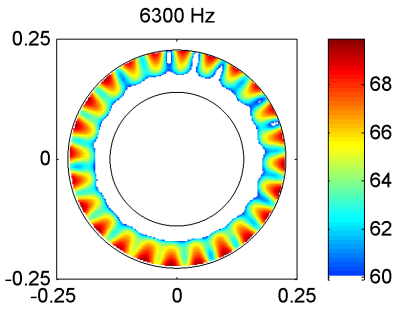

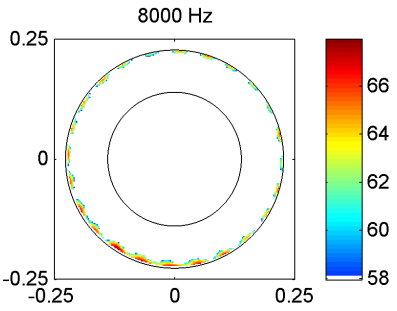

Problem area
The application of phased array beamforming inside turbofan engines ("in-duct beamforming") is relatively new. The feasibility to locate sources on rotor blades and stator vanes of a fan rig has been demonstrated recently. This was done with an existing intake circular microphone array, which is normally used for azimuthal mode detection. By "Conventional Beamforming" (CB), sources could be made visible on the stator.

Description of work
In this paper, Circular Harmonics Beamforming (CHB) is proposed as an alternative for CB in axisymmetric set-ups. In CHB the steering vectors are composed of azimuthal mode amplitudes rather than Green's function values. In order to obtain these amplitudes, microphones have to be arranged in rings.

Results and conclusions
An important feature of CHB is that the extension to rotating sources is straightforward and, therefore, easy to implement. Also the application to multiple rings of microphones is not too complicated.

Applicability
CHB can be applied to in-duct array measurements, when the microphones are mounted in rings, and stay away from bifurcations (radial splitters).

Report no.
NLR-TP-2012-247

Author(s)
P. Sijtsma

Report classification
UNCLASSIFIED

Date
July 2012

Knowledge area(s)
Aëro-akoestisch en experimenteel aërodynamisch onderzoek

Descriptor(s)
Engine Noise
Microphone Arrays

This report is based on a presentation held at the 18th AIAA/CEAS Aeroacoustics Conference, Colorado Srpings, CO, USA, 4-6 June 2012.

Circular Harmonics Beamforming with multiple rings of microphones
AIAA Paper 2012-2224

Nationaal Lucht- en Ruimtevaartlaboratorium, National Aerospace Laboratory NLR

Anthony Fokkerweg 2, 1059 CM Amsterdam,
P.O. Box 90502, 1006 BM Amsterdam, The Netherlands
Telephone +31 88 511 31 13, Fax +31 88 511 32 10, Web site: www.nlr.nl

Nationaal Lucht- en Ruimtevaartlaboratorium
National Aerospace Laboratory NLR

NLR-TP-2012-247

Circular Harmonics Beamforming with multiple rings of microphones

AIAA Paper 2012-2224

P. Sijtsma

This report is based on a presentation held at the 18th AIAA/CEAS Aeroacoustics Conference, Colorado Srpings, CO, USA, 4-6 June 2012.

Customer	National Aerospace Laboratory NLR
Contract number	GA 213411
Owner	National Aerospace Laboratory NLR
Division NLR	Aerospace Vehicles
Distribution	Unlimited
Classification of title	Unclassified
	July 2012

Approved by:

Author	Reviewer	Managing department
P. Sijtsma	M. Oppeneer	J. Hakkaart
Date:	Date:	Date:

Contents

Circular Harmonics Beamforming with Multiple Rings of Microphones

Pieter Sijtsma*
National Aerospace Laboratory NLR, 8300 AD Emmeloord, The Netherlands

Circular Harmonics Beamforming (CHB) is proposed as an alternative for Conventional Beamforming (CB) in axisymmetric set-ups. In CHB the steering vectors are composed of azimuthal mode amplitudes rather than Green's function values. In order to obtain these amplitudes, microphones have to be arranged in rings. An important feature of CHB is that the extension to rotating sources is straightforward and, therefore, easy to implement. Also the application to multiple rings of microphones is not too complicated. Thus, CHB can be applied to in-duct array measurements, when the microphones are mounted in rings, and stay away from bifurcations. Apart from a general discussion about the CHB method, this paper considers a few applications to simulated and measured in-duct array measurements.

Nomenclature

CB	=	Conventional Beamforming
CHB	=	Circular Harmonics Beamforming
CSM	=	Cross-Spectral Matrix
A	=	source auto-power
a	=	source amplitude
$\mathbf{C}$	=	cross-spectral matrix
C_{mn}	=	microphone cross-power
c_0	=	ambient sound speed
d	=	liner thickness
F_k	=	axial Fourier transform of G_k
$\mathbf{G}$	=	see Eq. (37)
G_k	=	azimuthal mode of Green's function
$\mathbf{g}$	=	steering vector
g_n	=	steering vector component
$\mathbf{H}$	=	see Eq. (37)
$H_k^{(2)}$	=	k-th order Hankel function of the second kind
$\mathbf{h}$	=	mode spectrum of steering vector
$\tilde{\mathbf{h}}$	=	see Eq. (31)
h_k	=	azimuthal mode amplitude of steering vector
$\tilde{h}_k$	=	see Eq. (31)
i	=	imaginary unit
J	=	cost function
J_k	=	k-th order Bessel function (of the first kind)
K	=	maximum azimuthal mode number
k	=	azimuthal mode number
L	=	number of microphone rings
l	=	microphone ring index
M	=	axial flow Mach number
m	=	microphone index

* Senior Scientist, Department of Helicopters & Aeroacoustics, P.O. Box 153, Member AIAA.

N = number of microphones
n = microphone index
$\mathbf{P}$ = see Eq. (37)
$\mathbf{p}$ = pressure vector
p_n = complex pressure amplitude
$\mathbf{Q}$ = see Eq. (37)
$\mathbf{q}$ = measured azimuthal mode spectrum
$\tilde{\mathbf{q}}$ = see Eq. (31)
q_k = measured azimuthal mode amplitude
$\tilde{q}_k$ = see Eq. (31)
r = radial coordinate
$\mathbf{T}$ = see Eq. (20)
t = time
U = main flow velocity
$V_{k\mu}$ = radial eigenfunction
x = axial coordinate
$\vec{x}_n$ = microphone location
Z = dimensionless wall impedance

α = axial wave number
β^2 = see Eq. (14)
$\beta_{k\mu}(\omega)$ = see Eq. (13)
δ = Dirac-delta function.
ε = radial wave number, see Eq. (11)
$\varepsilon_{k\mu}$ = radial eigenvalue
ϕ = azimuthal coordinate of source
μ = radial mode number
θ = azimuthal coordinate
ρ = radial coordinate of source
Ω = rotation speed
ω = angular frequency
ξ = axial coordinate of source
$\vec{\xi}$ = source location

I. Introduction

THE application of phased array beamforming inside turbofan engines ("in-duct beamforming") is relatively new. The feasibility to locate sources on rotor blades and stator vanes of a fan rig has been demonstrated recently[1-3]. This was done with an existing intake circular microphone array, which is normally used for azimuthal mode detection. By "Conventional Beamforming" (CB), sources could be made visible on the stator. Furthermore, by beamforming with rotating focus, sources were visualized on the rotor.

In the above-mentioned applications of in-duct beamforming use was made of free-field Green's functions to construct the so-called "steering vectors". This means that wall-reflections were ignored. To reduce the effects of these reflections, the measurements were carried out with an intake liner. A different beamforming approach was followed by Lowis and Joseph[4], who included duct wall reflections in the Green's function. Dougherty et al[5-6] applied steering vectors based on duct modes, instead of using Green's functions.

In the references cited above, several methods were used to locate rotating sources. Sijtsma[1-3] applied the rotating beamformer ROSI[7], which was originally developed for wind turbine blades. For in-duct applications, Lowis and Joseph[4] developed the "Rotating Focused Beamformer" and Dougherty and Walker[5] introduced "Virtual Rotating Microphone Imaging". Each of these methods are generalizations of CB, and not easy to understand.

Recently Tiana-Roig, Jacobsen, and Fernández Grande[8] introduced the concept of "Circular Harmonics Beamforming" (CHB), as an alternative for CB in an axisymmetric set-up. The difference with CB is that the steering vectors are composed of azimuthal mode amplitudes instead of Green's function values. The intended application of CHB was environmental noise, but the method can be applied to in-duct array measurements as well,

as long as the set-up is axisymmetric. In other words, the microphones need to be mounted in rings, and stay away from bifurcations (radial splitters).

There is no reason to expect with CHB better or worse results than with CB. However, an important feature is that extension to rotating sources is straightforward and, therefore, easy to implement. Also the application to multiple rings of microphones is not too complicated.

In this paper, the CHB method is discussed, including the extension to multiple rings. Further, the application of the method to simulated and measured array data is considered. For reference, the CB method is reviewed first.

II. Conventional Beamforming

We start from complex pressure amplitudes in the frequency domain, $p_n(\omega)$, measured by microphones located at positions $\vec{x}_n$, $n = 1,...,N$. For convenience, the pressure amplitudes are put into an N-dimensional vector:

$$\mathbf{p}(\omega) = \begin{pmatrix} p_1(\omega) \\ \vdots \\ p_N(\omega) \end{pmatrix}. \tag{1}$$

The source description is put in the "steering vector" $\mathbf{g}(\omega)$, i.e., its components $g_n(\omega)$ are the pressure amplitudes at the microphone locations of an ideal source with unit strength.

The aim of beamforming is to determine complex amplitudes $a(\omega)$ of sources in $\vec{\xi}$. This is done by comparing the measured pressure vector $\mathbf{p}(\omega)$ with the steering vector $\mathbf{g}(\omega)$ through minimization of

$$J = \left\| \mathbf{p}(\omega) - a(\omega)\mathbf{g}(\omega) \right\|^2. \tag{2}$$

The solution of this minimization problem is

$$a(\omega) = \frac{\mathbf{g}^*(\omega)\mathbf{p}(\omega)}{\left\| \mathbf{g}(\omega) \right\|^2}, \tag{3}$$

where the asterisk denotes complex conjugate transposition. Source auto-spectra are given by

$$A(\omega) = \frac{1}{2} a(\omega) a^*(\omega) = \frac{1}{2} \frac{\mathbf{g}^*(\omega)\mathbf{p}(\omega)\mathbf{p}^*(\omega)\mathbf{g}(\omega)}{\left\| \mathbf{g}(\omega) \right\|^4}. \tag{4}$$

Averaging over several blocks of data gives

$$A(\omega) = \frac{\mathbf{g}^*(\omega)\mathbf{C}(\omega)\mathbf{g}(\omega)}{\left\| \mathbf{g}(\omega) \right\|^4}, \tag{5}$$

in which the "Cross-Spectral Matrix" (CSM) is introduced:

$$\mathbf{C}(\omega) = \frac{1}{2} \left\langle \mathbf{p}(\omega)\mathbf{p}^*(\omega) \right\rangle. \tag{6}$$

In many cases, "cleaner" noise maps are obtained when the main diagonal of the CSM is excluded from the beamforming process. For that purpose, the following alternative can be used:

$$A(\omega) = \frac{\sum_{m=1}^{N}\sum_{n=1}^{N} g_m^*(\omega) C_{mn}(\omega) g_n(\omega) - \sum_{n=1}^{N} C_{nn}(\omega) \left| g_n(\omega) \right|^2}{\left(\sum_{n=1}^{N} \left| g_n(\omega) \right|^2 \right)^2 - \sum_{n=1}^{N} \left| g_n(\omega) \right|^4}. \tag{7}$$

III. Circular Harmonics Beamforming

A. Decomposition in circular harmonics

For CHB it is required that the steering vector components can be written like

$$g_n(\omega) = \sum_{k=-\infty}^{\infty} \exp\left[-ik(\theta_n - \phi) \right] G_k(\omega, x_n, r_n, \xi, \rho), \tag{8}$$

where (x_n, r_n, θ_n) are the microphone locations in cylindrical coordinates, and (ξ, ρ, ϕ) is the source location. If steering vectors are based on Green's function expressions, then Eq. (8) means that the Green's function is decomposed into azimuthal modes.

In a companion paper[9] a semi-analytical method is described to calculate G_k for a wide range of applications. For example, in a free field with uniform flow U and sound speed c_0 we have

$$G_k(\omega, x_n, r_n, \xi, \rho) = \frac{1}{2\pi}\int_{-\infty}^{\infty} \exp\left[i\alpha\left(x_n - \xi\right)\right] F_k(\omega, \alpha, r_n, \rho) d\alpha \,, \tag{9}$$

with

$$F_k(\omega, \alpha, r, \rho) = \frac{i}{4}\begin{cases} H_k^{(2)}(\varepsilon\rho) J_k(\varepsilon r), & r < \rho, \\ J_k(\varepsilon\rho) H_k^{(2)}(\varepsilon r), & r > \rho, \end{cases} \tag{10}$$

where J_k is the k-th order Bessel function, $H_k^{(2)}$ the k-th order Hankel function of the second kind, and

$$\varepsilon^2 = -\alpha^2 + \left(\omega + U\alpha\right)^2 / c_0^2 \,. \tag{11}$$

Another well-known example is the Green's function in an annular flow duct with hard walls[10]:

$$G_k(\omega, x_n, r_n, \xi, \rho) = \frac{-1}{4\pi i}\sum_{\mu=1}^{\infty} \frac{V_{k\mu}(\rho) V_{k\mu}(r_n)}{\beta_{k\mu}(\omega)} \times \begin{cases} \exp\left[i\alpha_{k\mu}^{+}\left(x_n - \xi\right)\right], & x_n > \xi, \\ \exp\left[i\alpha_{k\mu}^{-}\left(x_n - \xi\right)\right], & x_n < \xi, \end{cases} \tag{12}$$

where $\alpha_{k\mu}^{+-}$ are axial eigenvalues, $V_{k\mu}$ normalized eigenfunctions, and

$$\beta_{k\mu}(\omega) = \begin{cases} \left(\omega^2/c_0^2 - \beta^2\varepsilon_{k\mu}^2\right)^{1/2}, \text{ for } \beta^2\varepsilon_{k\mu}^2 < \omega^2/c_0^2 \,, \\ -i\left(\beta^2\varepsilon_{k\mu}^2 - \omega^2/c_0^2\right)^{1/2}, \text{ for } \beta^2\varepsilon_{k\mu}^2 \geq \omega^2/c_0^2 \,. \end{cases} \tag{13}$$

Further, $\varepsilon_{k\mu}$ are axial eigenvalues (related to the axial eigenvalues by Eq. (11)) and

$$\beta^2 = 1 - U^2/c_0^2 \,. \tag{14}$$

Dougherty et al[5,6] ignored the $\beta_{k\mu}(\omega)$ denominator in (12), thus avoiding resonance, which would make beamforming impossible.

B. Single ring of microphones

It is assumed that measurements are done with a circular "mode detection array":

$$\vec{x}_n = (x, r, \theta_n), \; n = 1, ..., N \,. \tag{15}$$

In other words, the axial and the radial coordinate of the microphone locations are fixed. Suppose that we can extract circular harmonics (i.e., azimuthal mode amplitudes) $q_k(\omega)$ from this array, so that we have

$$p_n(\omega) = \sum_{k=-\infty}^{\infty} q_k(\omega) \exp(-ik\theta_n) \,. \tag{16}$$

We have to compare the measured pressures with the steering vector components (8), for which we briefly write

$$g_n(\omega) = \sum_{k=-\infty}^{\infty} h_k(\omega) \exp\left(-ik\theta_n\right), \tag{17}$$

with

$$h_k(\omega) = \exp\left(ik\phi\right) G_k(\omega, x, r, \xi, \rho) \,. \tag{18}$$

The summations in (16) and (17) are truncated by replacing the "∞" symbol by K. Then we can write in vector-matrix notation:

$$\mathbf{p}(\omega) = \mathbf{T}\mathbf{q}(\omega), \; \mathbf{g}(\omega) = \mathbf{T}\mathbf{h}(\omega) \,, \tag{19}$$

where $\mathbf{T}$ is an $N\times(2K+1)$-matrix with

$$T_{nk} = \exp\left(-ik\theta_n\right) \,. \tag{20}$$

With CB we would solve the minimization problem

$$J = \left\|\mathbf{p}(\omega) - a(\omega)\mathbf{g}(\omega)\right\|^2 = \left\|\mathbf{T}\left\{\mathbf{q}(\omega) - a(\omega)\mathbf{h}(\omega)\right\}\right\|^2 \,. \tag{21}$$

The CHB method simplifies this to

$$J = \left\|\mathbf{q}(\omega) - a(\omega)\mathbf{h}(\omega)\right\|^2 \,. \tag{22}$$

The solution is

$$a(\omega)=\frac{\mathbf{h}^*(\omega)\mathbf{q}(\omega)}{\|\mathbf{h}(\omega)\|^2}=\frac{\sum_{k=-K}^{K}h_k^*(\omega)q_k(\omega)}{\sum_{k=-K}^{K}|h_k(\omega)|^2}. \tag{23}$$

Note that (21) and (22) are equivalent when an equidistant microphone array is used and $K=N/2$. In that case, the matrix **T** is unitary, apart from a factor $N^{1/2}$.

Tiana-Roig, Jacobsen, and Fernández Grande[8] implemented CHB slightly differently:

$$a(\omega)=\frac{1}{2K+1}\sum_{k=-K}^{K}\frac{q_k(\omega)}{h_k(\omega)}. \tag{24}$$

When evanescent modes are included, this method lacks robustness. Therefore, this implementation is not considered here.

C. Rotating sources

For a rotating source at $(\xi,\rho,\phi+\Omega t)$, with source amplitude $a(\omega)$, it can be shown[4] that the induced pressures are

$$g(\omega)=\sum_{k=-\infty}^{\infty}a(\omega-k\Omega)\exp\left[-ik\left(\theta-\phi\right)\right]G_k(\omega,x,r,\xi,\rho). \tag{25}$$

For a single-frequency source at unit strength, i.e., for

$$a(\omega)=\delta(\omega-\omega_0), \tag{26}$$

we have

$$g(\omega)=\sum_{k=-\infty}^{\infty}\delta\left(\omega-(\omega_0+k\Omega)\right)\exp\left[-ik\left(\theta-\phi\right)\right]G_k(\omega_0+k\Omega,x,r,\xi,\rho). \tag{27}$$

Hence, there is scattering to frequencies $\omega_0+k\Omega$.

Just like Eq. (17) we can write for the steering vector components:

$$g_n(\omega_0)=\sum_{k=-\infty}^{\infty}h_k(\omega_0+k\Omega)\exp\left(-ik\theta_n\right), \tag{28}$$

which has to be compared to the measured counterpart:

$$p_n(\omega_0)=\sum_{k=-\infty}^{\infty}q_k(\omega_0+k\Omega)\exp(-ik\theta_n). \tag{29}$$

In vector-matrix notation, and omitting the subscript "0", we write

$$\mathbf{p}(\omega)=\mathbf{T}\tilde{\mathbf{q}}(\omega),\ \mathbf{g}(\omega)=\mathbf{T}\tilde{\mathbf{h}}(\omega), \tag{30}$$

with

$$\tilde{h}_k(\omega)=h_k(\omega+k\Omega),\ \tilde{q}_k(\omega)=q_k(\omega+k\Omega). \tag{31}$$

Analogously to the previous section, CB would mean the minimization of

$$J=\|\mathbf{p}(\omega)-a(\omega)\mathbf{g}(\omega)\|^2=\left\|\mathbf{T}\left\{\tilde{\mathbf{q}}(\omega)-a(\omega)\tilde{\mathbf{h}}(\omega)\right\}\right\|^2, \tag{32}$$

while for the CHB method the cost function is

$$J=\left\|\tilde{\mathbf{q}}(\omega)-a(\omega)\tilde{\mathbf{h}}(\omega)\right\|^2. \tag{33}$$

The solution of minimizing (33) is

$$a(\omega)=\frac{\tilde{\mathbf{h}}^*(\omega)\tilde{\mathbf{q}}(\omega)}{\left\|\tilde{\mathbf{h}}(\omega)\right\|^2}. \tag{34}$$

D. Multiple rings

If there is more than one ring of microphones, say

$$\vec{x}_{ln}=(x_l,r,\theta_{ln}),\ n=1,\ldots,N_l,\ l=1,\ldots,L, \tag{35}$$

then we can generalize the minimization problem (21), (22) to

$$J = \left\|\mathbf{P}(\omega) - a(\omega)\mathbf{G}(\omega)\right\|^2 = \sum_{l=1}^{L}\left\|\mathbf{p}_l(\omega) - a(\omega)\mathbf{g}_l(\omega)\right\|^2 = \sum_{l=1}^{L}\left\|\mathbf{T}_l\left(\mathbf{q}_l(\omega) - a(\omega)\mathbf{h}_l(\omega)\right)\right\|^2$$
$$\approx \sum_{l=1}^{L} N_l \left\|\mathbf{q}_l(\omega) - a(\omega)\mathbf{h}_l(\omega)\right\|^2 = \left\|\mathbf{Q}(\omega) - a(\omega)\mathbf{H}(\omega)\right\|^2 \tag{36}$$

with

$$\mathbf{P}(\omega) = \begin{pmatrix}\mathbf{p}_1(\omega)\\ \vdots \\ \mathbf{p}_L(\omega)\end{pmatrix},\ \mathbf{G}(\omega) = \begin{pmatrix}\mathbf{g}_1(\omega)\\ \vdots \\ \mathbf{g}_L(\omega)\end{pmatrix},\ \mathbf{Q}(\omega) = \begin{pmatrix}N_1^{1/2}\mathbf{q}_1(\omega)\\ \vdots \\ N_L^{1/2}\mathbf{q}_L(\omega)\end{pmatrix},\ \mathbf{H}(\omega) = \begin{pmatrix}N_1^{1/2}\mathbf{h}_1(\omega)\\ \vdots \\ N_L^{1/2}\mathbf{h}_L(\omega)\end{pmatrix}. \tag{37}$$

The number of microphones N_l and the mode range $-K_l \le k \le K_l$ may differ from ring to ring. The solution of (36) is

$$a(\omega) = \frac{\mathbf{H}^*(\omega)\mathbf{Q}(\omega)}{\left\|\mathbf{H}(\omega)\right\|^2} = \frac{\sum_{l=1}^{L} N_l \mathbf{h}_l^*(\omega)\mathbf{q}_l(\omega)}{\sum_{l=1}^{L} N_l \left\|\mathbf{h}_l(\omega)\right\|^2}. \tag{38}$$

For rotating sources, the extension to multiple rings is analogous.

E. Source auto-spectra

In this section, we discuss a few aspects of source auto-spectra calculation. This is done for single rings only. The extension to multiple rings is straightforward. Source auto-spectra $A(\omega)$ are calculated by squaring the source amplitude $a(\omega)$. For example, with (23) we obtain:

$$A(\omega) = \frac{1}{2}\left|a(\omega)\right|^2 = \frac{\mathbf{h}^*(\omega)\left\{\frac{1}{2}\mathbf{q}(\omega)\mathbf{q}^*(\omega)\right\}\mathbf{h}(\omega)}{\left\|\mathbf{h}(\omega)\right\|^4}. \tag{39}$$

Averaging can be applied to the mode CSM: $\mathbf{q}(\omega)\mathbf{q}^*(\omega)/2$. If the spectrum is evaluated in engine orders, then the phase locked tones can be filtered out by subtracting $\langle\mathbf{q}(\omega)\rangle\langle\mathbf{q}(\omega)\rangle^*/2$ from $\langle\mathbf{q}(\omega)\mathbf{q}^*(\omega)\rangle/2$.

The mode amplitudes can be estimated from the array spectra by[11]

$$\mathbf{q}(\omega) = \frac{1}{N}\mathbf{T}^*\mathbf{p}(\omega). \tag{40}$$

Hence, the mode CSM can be estimated from the array CSM by

$$\frac{1}{2}\mathbf{q}(\omega)\mathbf{q}^*(\omega) = \frac{1}{2N^2}\mathbf{T}^*\mathbf{p}(\omega)\mathbf{p}^*(\omega)\mathbf{T} = \frac{1}{N^2}\mathbf{T}^*\mathbf{C}(\omega)\mathbf{T}. \tag{41}$$

If removal of auto-spectra is required, we can replace (41) by

$$\frac{1}{2}\mathbf{q}(\omega)\mathbf{q}^*(\omega) = \frac{1}{N(N-1)}\mathbf{T}^*\bar{\mathbf{C}}(\omega)\mathbf{T}, \tag{42}$$

where $\bar{\mathbf{C}}$ is the "trimmed" array CSM, in which the diagonal elements are replaced by zeros.

For rotating sources, we obtain

$$A(\omega) = \frac{\tilde{\mathbf{h}}^*(\omega)\left\{\frac{1}{2}\tilde{\mathbf{q}}(\omega)\tilde{\mathbf{q}}^*(\omega)\right\}\tilde{\mathbf{h}}(\omega)}{\left\|\tilde{\mathbf{h}}(\omega)\right\|^4}, \tag{43}$$

with

$$\left\{\frac{1}{2}\tilde{\mathbf{q}}(\omega)\tilde{\mathbf{q}}^*(\omega)\right\}_{k_1k_2} = \frac{1}{2N^2}\sum_{n=1}^{N}\sum_{m=1}^{N} T_{k_1n}^* p_n(\omega + k_1\Omega)\, p_m^*(\omega + k_2\Omega) T_{k_2m}. \tag{44}$$

From this expression we can eliminate auto-spectra as well, but only if $k_1 = k_2$:

$$\left\{\frac{1}{2}\tilde{\mathbf{q}}(\omega)\tilde{\mathbf{q}}^*(\omega)\right\}_{kk} = \frac{1}{2N(N-1)}\left\{\sum_{n=1}^{N}\sum_{m=1}^{N} T_{kn}^* p_n(\omega + k\Omega)\, p_m^*(\omega + k\Omega) T_{km} - \sum_{n=1}^{N}\left|T_{kn}^* p_n(\omega + k\Omega)\right|^2\right\}. \tag{45}$$

IV. Applications

A. Simulation with cage array

Simulations were made with a "cage array" consisting of 4 rings of 25 microphones in a flow duct of 80 cm diameter. The microphone locations are shown in Figure 1. A uniform flow with Mach number $M = U/c_0 = 0.4$ is assumed. Furthermore, a stationary monopole point source was simulated in $(x, y, z) = (0, 0.32, 0)$. Array data were synthesized using a Green's function formulation for a lined hollow duct[9,12]. For the dimensionless wall-impedance we used

$$Z = 2.5 - i\cot\left(\omega d/c_0\right), \tag{46}$$

with liner cell thickness $d = 1$ cm. Beamforming was done on a scan plane through the source location, perpendicular to the axis, hence at $x = 0$. The free field Green's function was used to define the steering vectors. Beamforming with diagonal removal was applied. Reference results obtained with CB are plotted in Figure 2. Results are shown for frequencies ranging from 1500 Hz to 5500 Hz.

First, CHB was applied with maximum absolute azimuthal mode numbers $K_l = 12$. This is the maximum mode number that can be detected with these microphone rings, without aliasing[11]. The results, which are shown in Figure 3, start to differ from the CB results at frequencies higher than 2000 Hz. This is not surprising, as the range of (hard-wall) propagating modes is then significantly larger than $-12 \le k \le 12$.

In Figure 4 the maximum mode number was increased to $K_l = 18$. In other words, it was accepted that mode aliasing occurred. Now the images are equal to the CB images up to 3000 Hz, that is, as long as the propagating modes are within the range $-21 \le k \le 21$. In other words, it pays off to accept aliasing. In Figure 5 the maximum mode number was further increased to $K_l = 36$. Now the results are completely identical to the CB results.

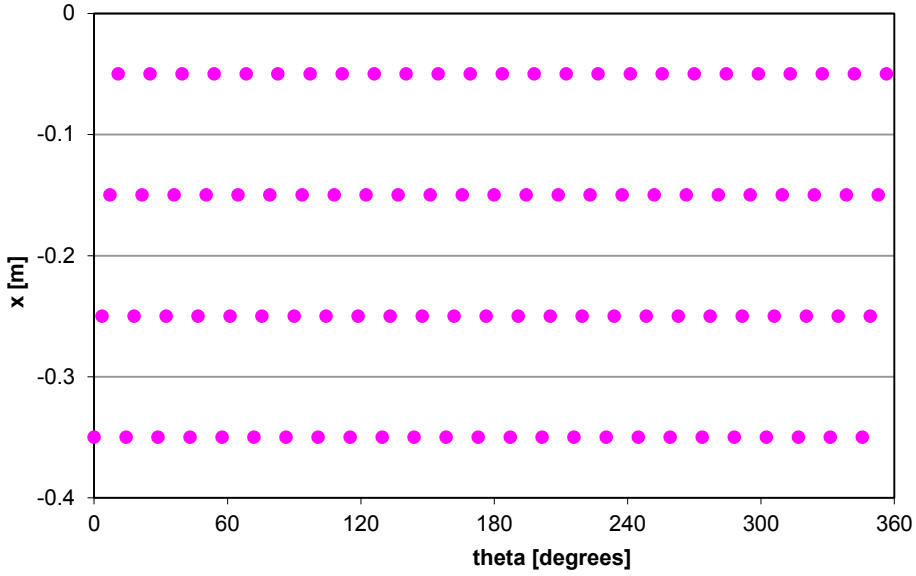

Figure 1. Cage array geometry.

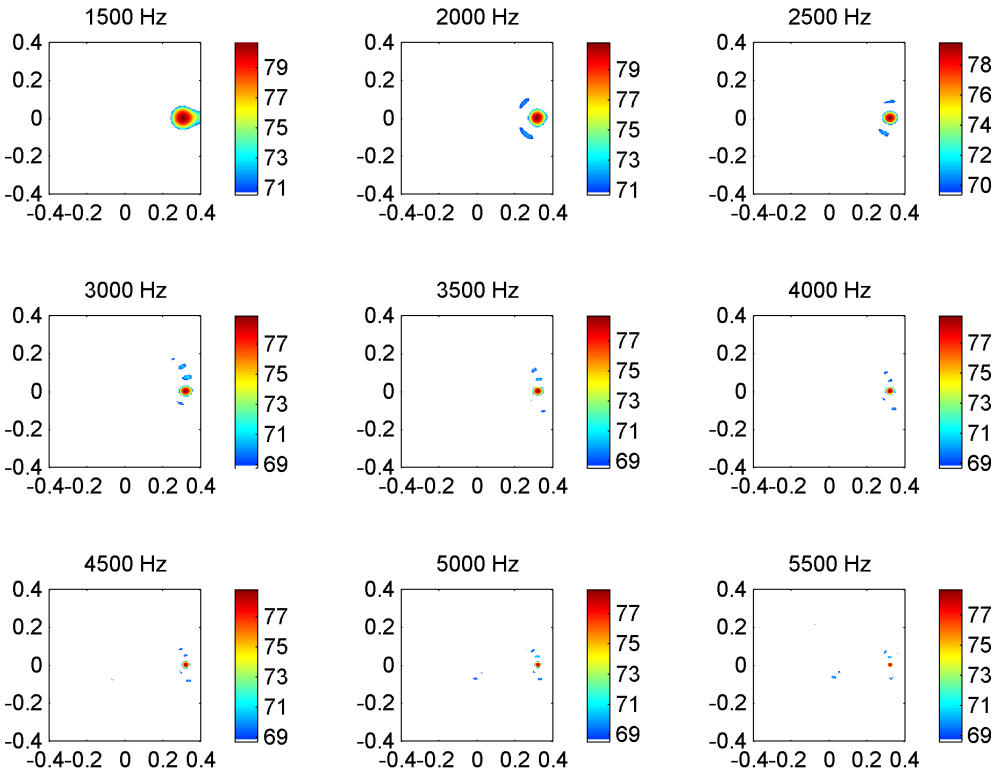

Figure 2. Acoustic images obtained with synthesized array data and CB; stationary focus.

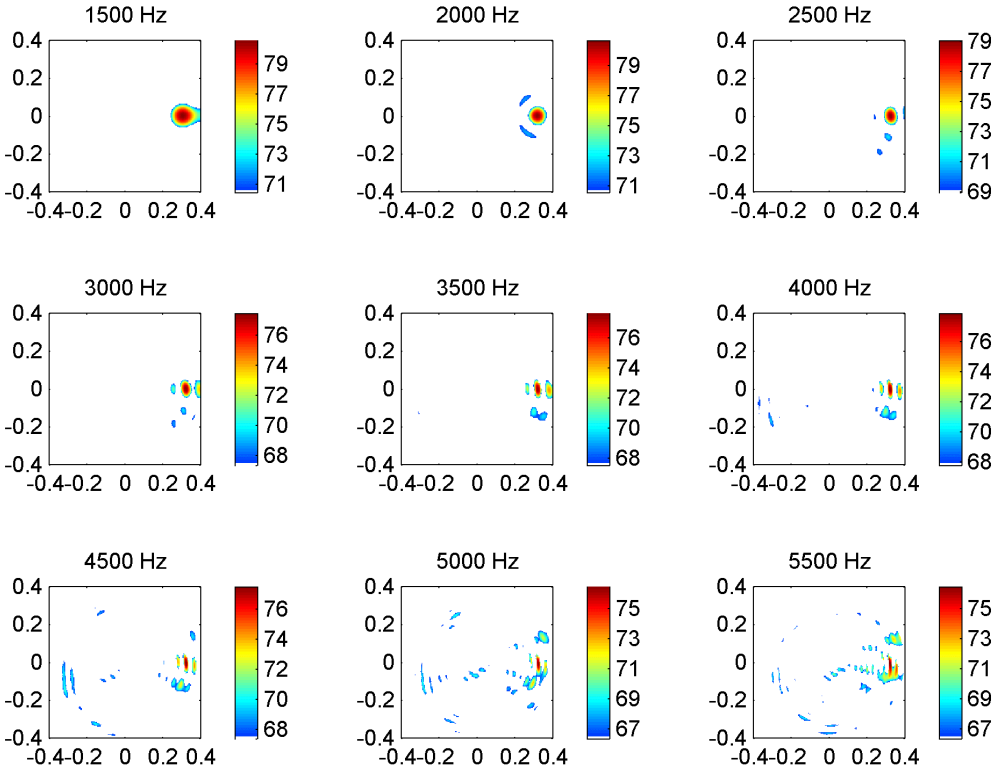

Figure 3. Acoustic images obtained with synthesized array data and CHB; maximum mode number $K_l = 12$; stationary focus.

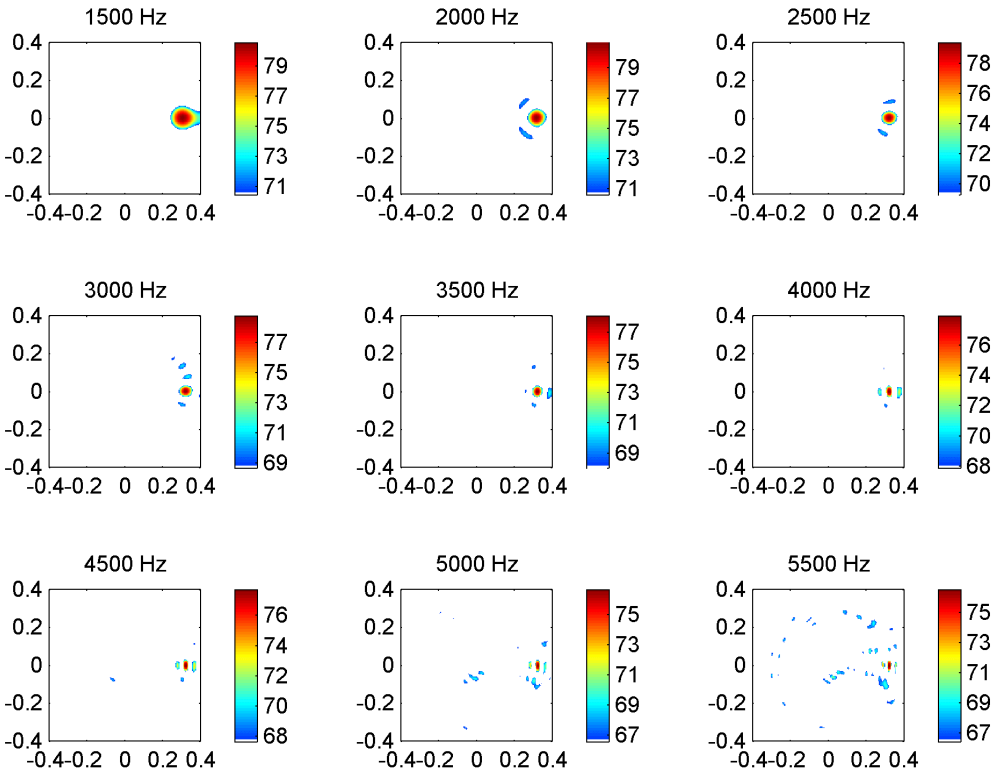

Figure 4. Acoustic images obtained with synthesized array data and CHB; maximum mode number $K_l = 18$; stationary focus.

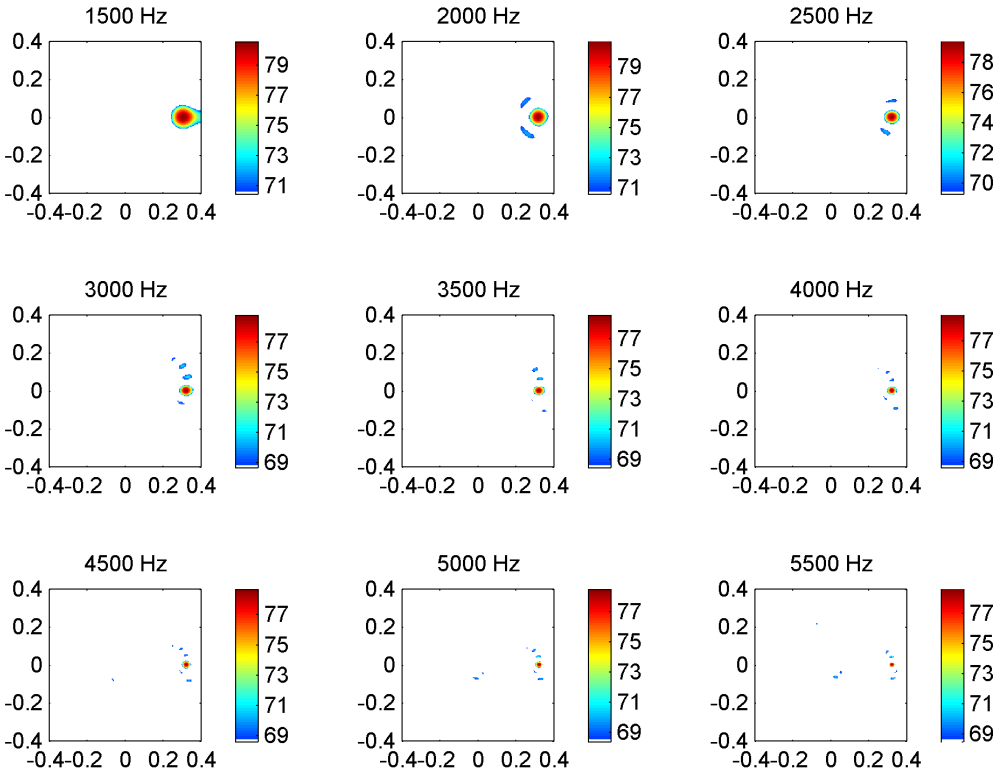

Figure 5. Acoustic images obtained with synthesized array data and CHB; maximum mode number $K_l = 36$; stationary focus.

B. Measurements on DLR fan model

CHB with rotating focus was applied to data measured with the DLR fan rig, which features a long intake duct of 45 cm diameter (see Figure 6). Upstream of the fan, a liner was installed. Upstream of the liner, an array was mounted consisting of 4 rings of microphones. Array measurements were done with the three downstream arrays (12, 12, and 36 microphones). For beamforming, we only used the downstream most array (36 microphones). Inclusion of the two smaller arrays did not change much with the results.

We show results here for a typical nominal fan operating condition. For modeling the sound propagation a uniform flow was assumed with Mach number $M = 0.047$. Rotor locked tones were filtered out.

Beamforming results are shown on a scan plane perpendicular to the axis, 38 cm downstream of the array. This location coincides, more or less, with the leading edges of the rotor blades. Acoustic images are shown at the 1/3 octave band frequencies 6300 Hz and 8000 Hz. At lower frequencies the beamforming resolution is too low to distinguish between the 24 rotor blades.

Figure 7 shows CHB results obtained with the free field Green's function, and without diagonal removal. The maximum mode number was set to $K = 32$, which is enough to capture the propagating modes at the frequencies of interest. Figure 8 shows the images obtained with diagonal removal. The images clearly show sources near the tips of the 24 rotor blades.

Figure 9 and Figure 10 show results obtained with a Green's function in a lined duct, without and with diagonal removal, respectively. Although the exact source distribution shown in these images looks questionable, the general observation remains the same, namely that acoustic sources appear near the rotor tips. Here, the maximum mode number was lower: $K = 17$. Higher values of K appeared to lead to loss of spatial resolution.

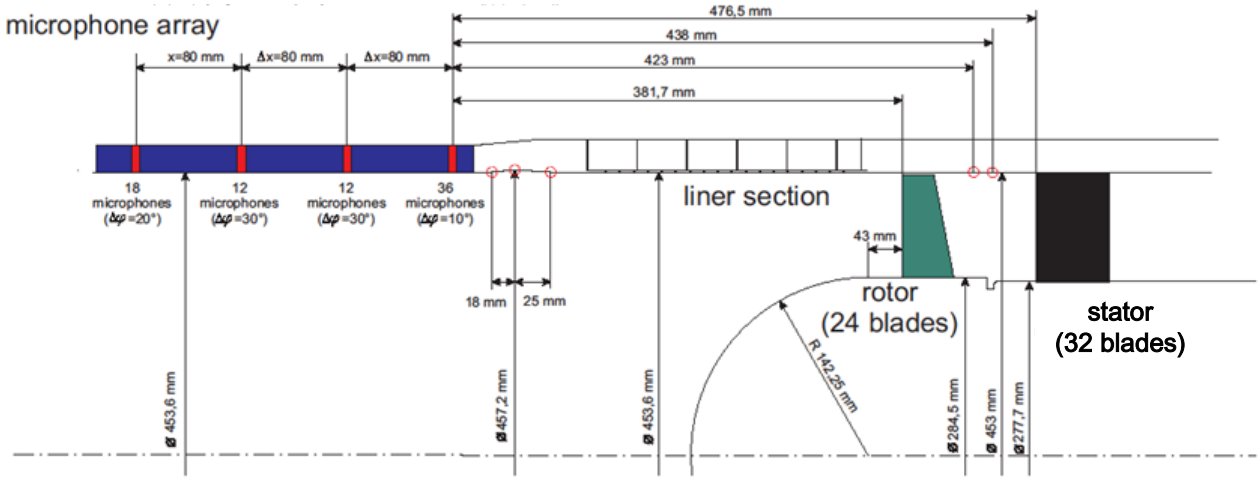

Figure 6. Intake of DLR fan rig.

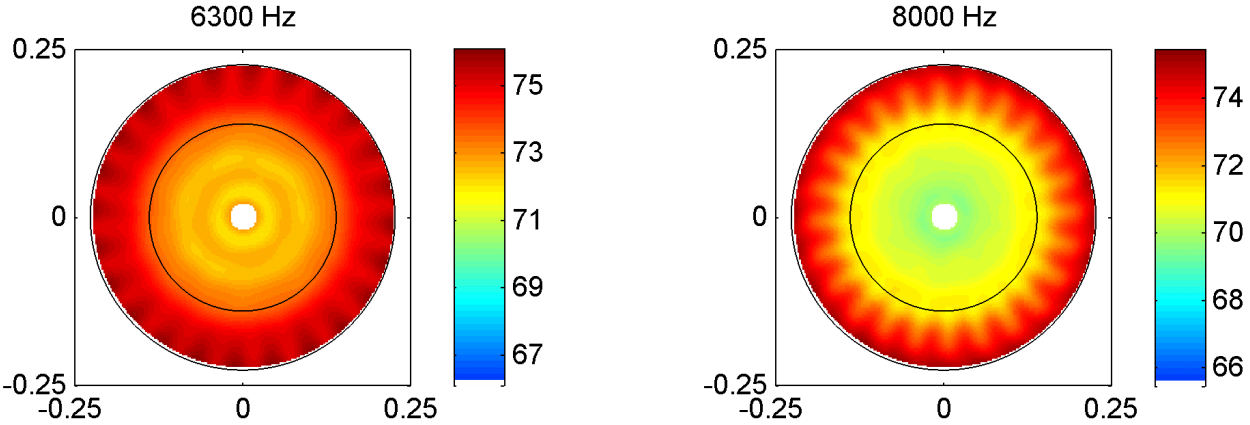

Figure 7. Acoustic images of DLR fan, obtained with CHB and rotating free field Green's function; no diagonal removal; maximum mode number $K = 32$.

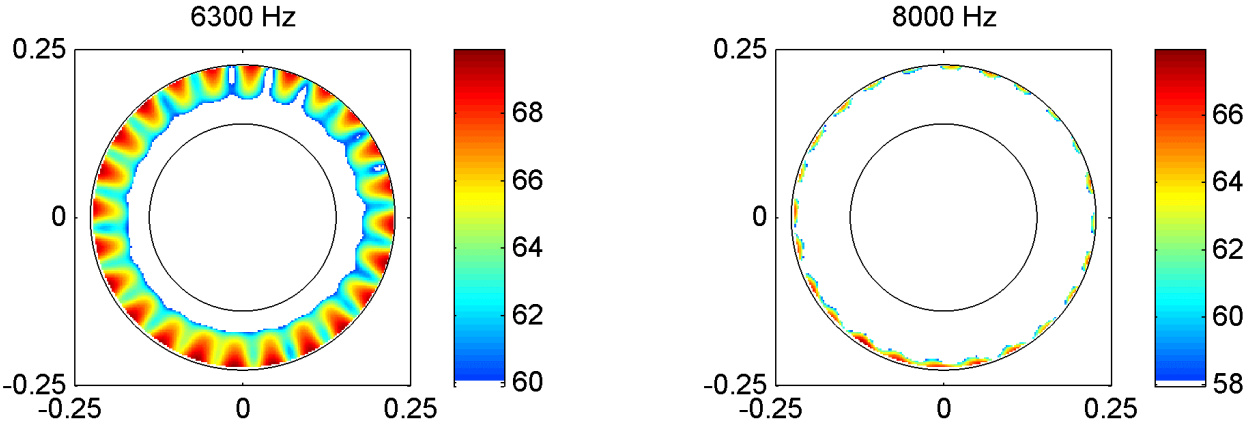

Figure 8. Acoustic images of DLR fan, obtained with CHB and rotating free field Green's function; with diagonal removal; maximum mode number $K = 32$.

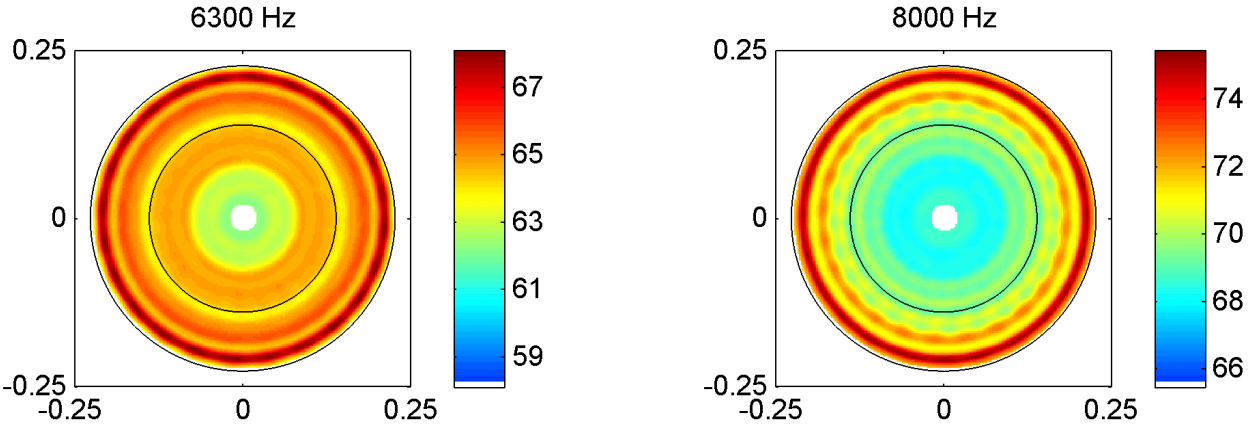

Figure 9. Acoustic images of DLR fan, obtained with CHB and rotating Green's function in lined duct; no diagonal removal; maximum mode number $K = 17$.

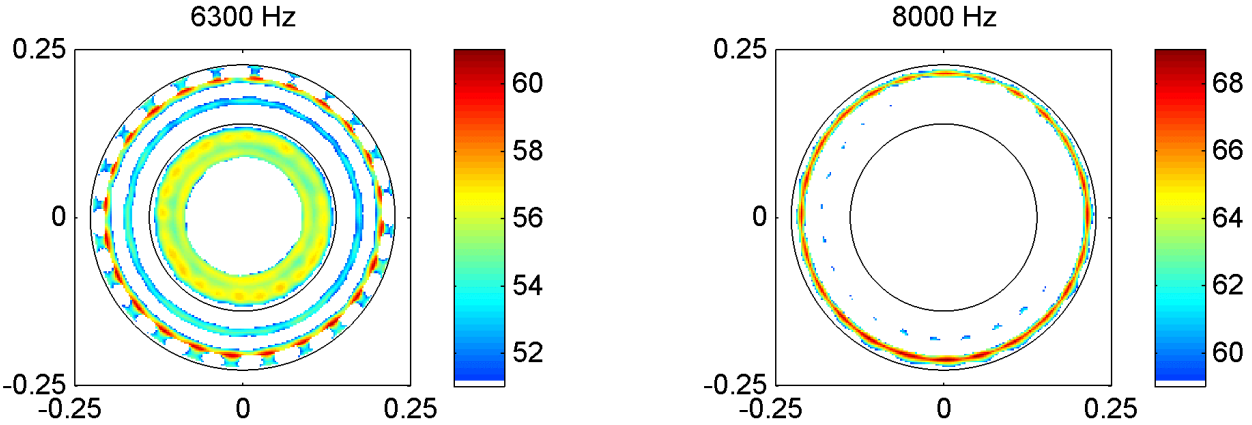

Figure 10. Acoustic images of DLR fan, obtained with CHB and rotating Green's function in lined duct; with diagonal removal; maximum mode number K = 17.

V. Conclusion

Circular Harmonics Beamforming is proposed as alternative for Conventional Beamforming in axisymmetric set-ups. CHB can be easily extended to rotating sources and multiple rings. Simulations with an array consisting of 4 microphone rings showed that the same results as CB can be obtained when mode aliasing is accepted. An application to measured in-duct array data showed the ability to locate rotating sources.

Acknowledgments

The investigations and the measurements reported in this paper were carried out within the project FLOCON, which is sponsored through the European Community's Seventh Framework Programme (FP7/2007-2013), under grant agreement n° 213411. Philip Kausche and Antoine Moreau of DLR Berlin are acknowledged for providing the measured data.

References

[1]Sijtsma, P., "Using Phased Array Beamforming to Locate Broadband Noise Sources inside a Turbofan Engine," AARC Engine Noise Phased Array Workshop, Cambridge, MA, 11-12 May 2006.

[2]Sijtsma, P., "Feasibility of In-Duct Beamforming", AIAA Paper 2007-3696, May 2007.

[3]Sijtsma, P., "Using Phased Array Beamforming to Identify Broadband Noise Sources in a Turbofan Engine," *International Journal of Aeroacoustics*, Vol. 9, No 3, 2010, pp. 357-374.

[4]Lowis, C. R., and Joseph, P., "A Focused Beamformer Technique for Separating Rotor and Stator-Based Broadband Sources," AIAA Paper 2006-2710, May 2006.

[5]Dougherty, R. P., and Walker, B. E., "Virtual Rotating Microphone Imaging of Broadband Fan Noise," AIAA Paper 2009-3121, May 2009.

[6]Dougherty, R. P., Walker, B. E., and Sutliff, D. L., "Locating and Quantifying Broadband Fan Sources Using In-Duct Microphones," AIAA Paper 2010-3736, June 2010.

[7]Sijtsma, P., Oerlemans, S., and Holthusen, H., "Location of Rotating Sources by Phased Array Measurements," AIAA Paper 2001-2167, May 2001.

[8]Tiana-Roig, E., Jacobsen, F., and Fernández Grande, E., "Beamforming with a Circular Microphone Array for Localization of Environmental Sound Sources," *Journal of the Acoustical Society of America*, Vol. 128, No. 6, 2010, pp. 3535-3542.

[9]Sijtsma, P., "Green's Functions for In-Duct Beamforming Applications," AIAA Paper 2012-2248, June 2012.

[10]Namba, M., "Three-Dimensional Analysis of Blade Force and Sound Generation for an Annular Cascade in Distorted Flow," *Journal of Sound and Vibration*, Vol. 50, No. 4, 1977, pp. 479-508.

[11]Rademaker, E. R., Sijtsma, P., and Tester, B. J., "Mode Detection with an Optimised Array in a Model Turbofan Engine Intake at Varying Shaft Speeds," AIAA Paper 2001-2181, 2001.

[12]Rienstra, S. W., and Tester, B. J., "An Analytic Green's Function for a Lined Circular Duct Containing Uniform Mean Flow," AIAA Paper 2005-3020, May 2005.